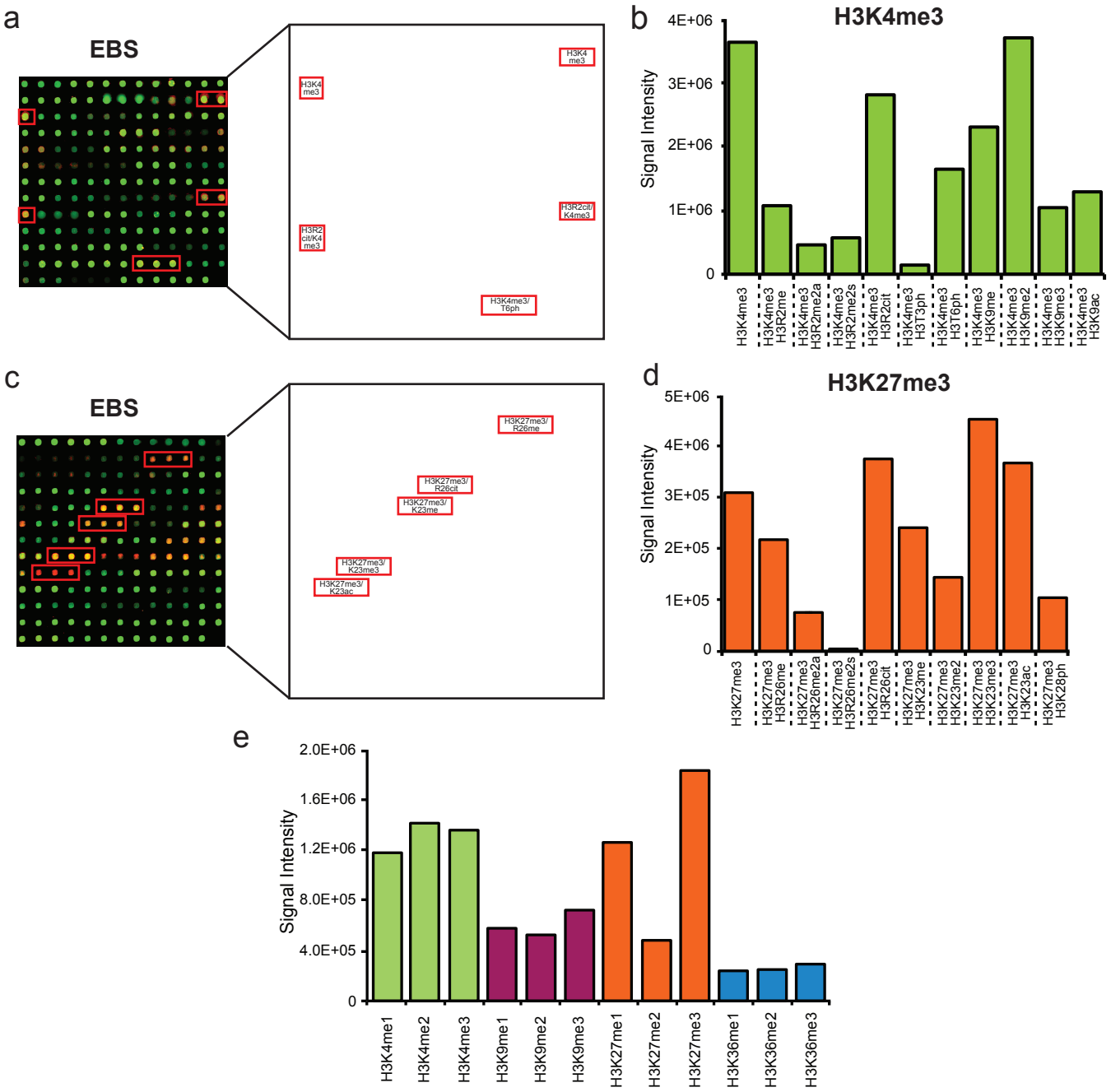

Supplementary Figure 1 EBS specifically binds methylated H3K4 and H3K27 marks. (**a,c**) Systematic profiling of histone binding preferences of full-length GST-EBS on a histone peptide microarray. A representative array image showing EBS binding to H3K4me3 (a) and H3K27me3 (c). (**b,d**) Relative intensity of selective H3K4me3-containing (b) and H3K27me3-containing (d) peptide species. Relative signal intensity is calculated by normalizing each mean signal intensity at 635 nm of triplicate spots to the highest signal on individual subarray, after subtracting background signals (derived from empty spots) for all spots. (**e**) Relative intensity of EBS binding with different peptides. Peptide species containing same PTMs are grouped together.

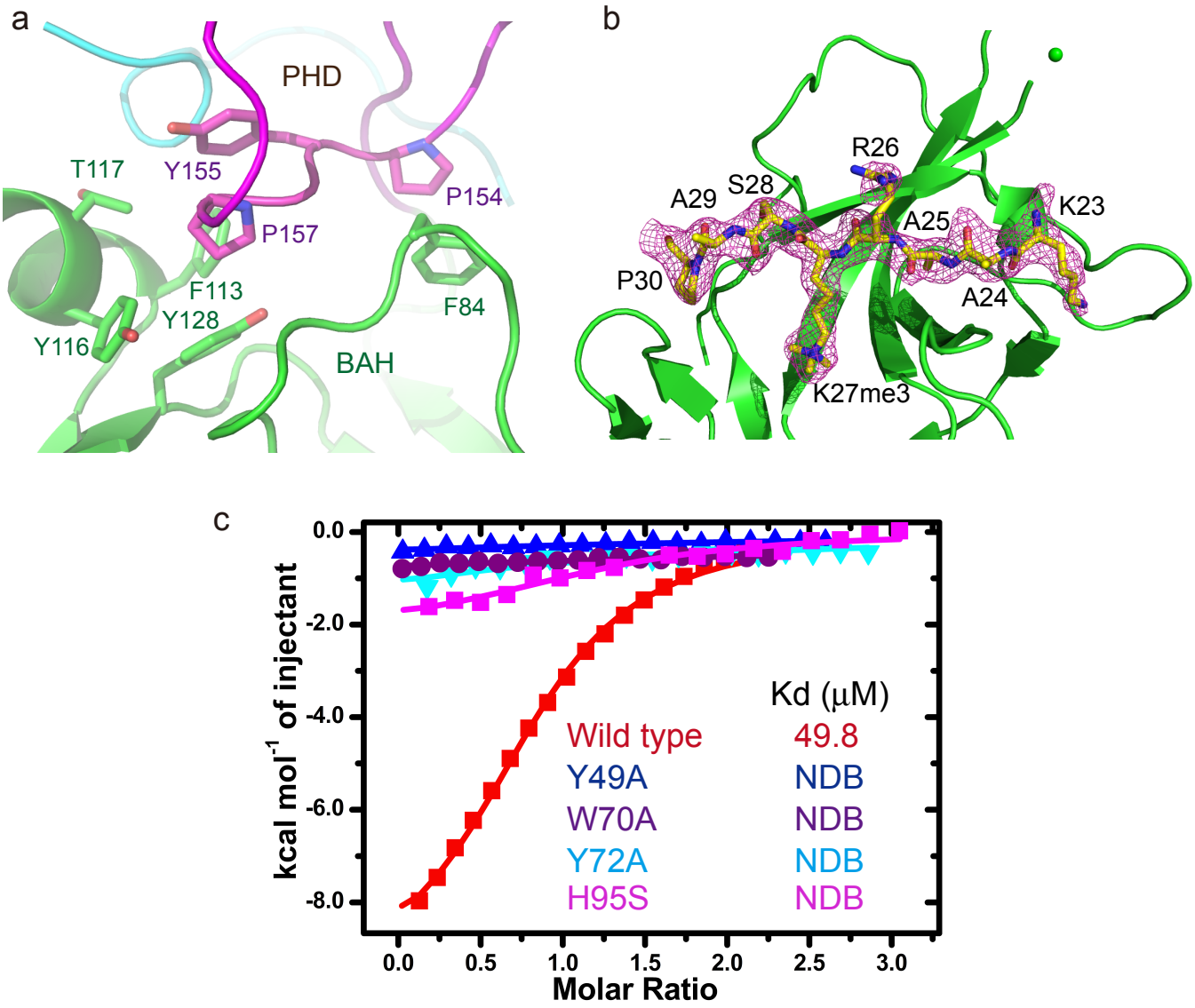

Supplementary Figure 2 Structural basis of EBS-H3K27me3 complex. (**a**) The interaction between BAH and PHD domians. The interacting residues are hight-lighted in the stick representation. (**b**) An omit map for the H3K27me3 peptide is shown in magenta mesh. (**c**) The ITC binding curves between H3K27me3 and various EBS point mutants revealing that the aromatic residues and His95 are essential for the recognition of H3K27me3. The ITC experiments were repeated twice independently with similar results.

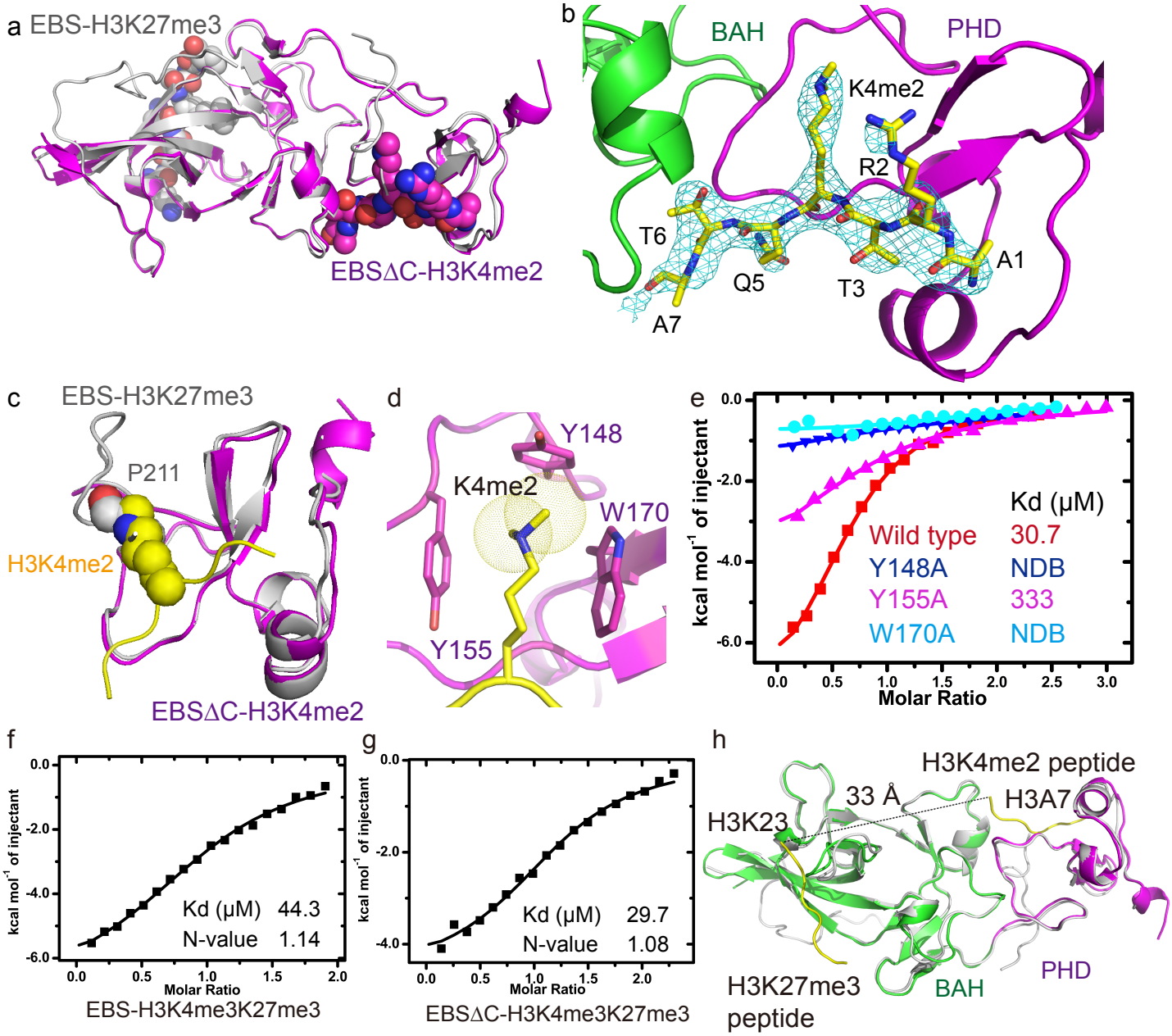

Supplementary Figure 3 The structure basis of EBSΔC in complex with H3K4me2 peptide. (**a**) The superposition of EBSΔC-H3K4me2 complex (in magenta) with EBS-H3K27me3 complex (in silver) showing that they have similar overall structures. The two peptides are shown in a space filling representation. (**b**) An omit map for the H3K4me2 peptide is shown in a cyan mesh. (**c**) The superposition of the two structures reveals that the Pro211 of C-terminal loop overlaps with H3K4me2, resulting in an auto-inhibition mode that blocks the binding of H3K4me3/2. (**d**) An enlarged view of the aromatic cage that accommodates H3K4me2. (**e**) The ITC binding curves between H3K4me3 and various EBS mutants revealing that the aromatic cage is essential for the H3K4me3 binding. (**f**) The ITC binding curves between EBS and a doubly methylated H3(1-35)K4me3K27me3 peptide. (**g**) The ITC binding curves between EBSΔC and a doubly methylated H3(1-35)K4me3K27me3 peptide. N values in f and g represent the binding stoichiometry. The ITC experiments were repeated twice independently with similar results. **(h)** A superposition of EBSΔC-H3K4me2 complex (in color) with EBS-H3K27me3 complex (in silver). The distance between H3A7 and H3K23 are measured to be 33 Å, which is hard to accomodate the spaning 15 reisudes considering the orentations of the two peptides. Thus, EBS prefers to bind the H3K4me3 and H3k27me3 indenpendently but not simultaneously.

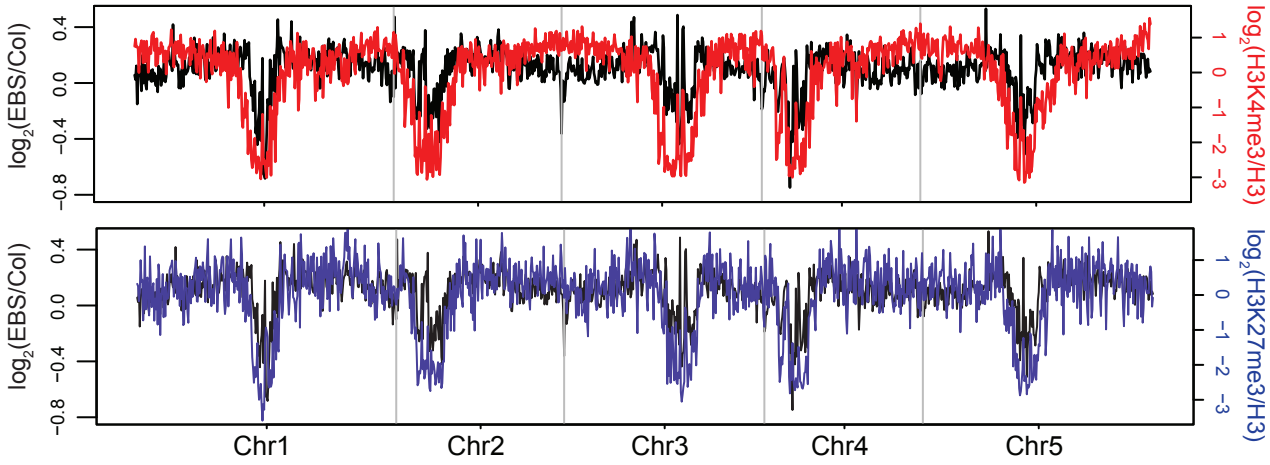

Supplementary Figure 4 Chromosomal views show that EBS are co-localized with H3K4me3 (red) and H3K27me3 (blue) along five Arabidopsis chromosomes.

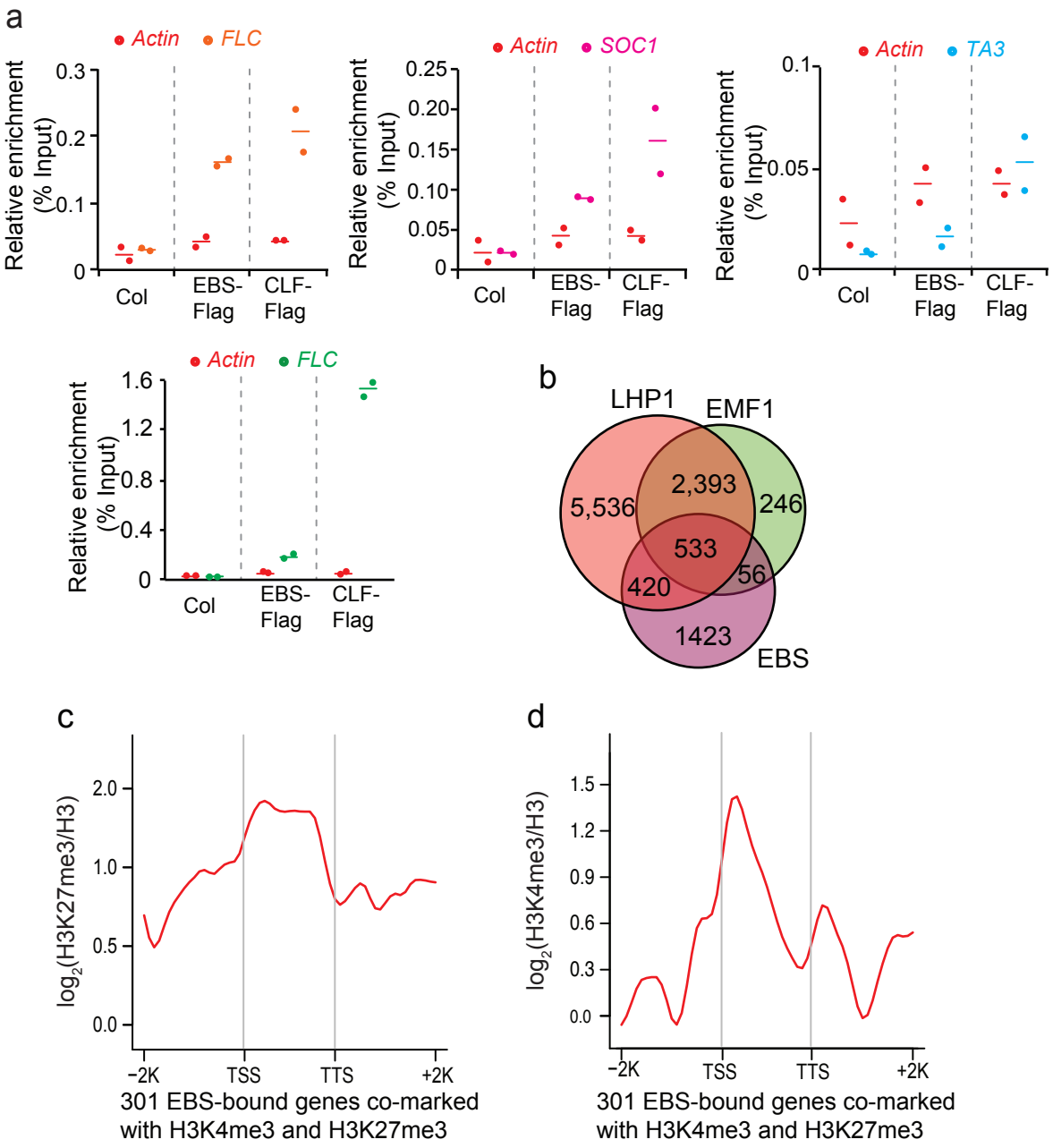

Supplementary Figure 5 EBS and PRC proteins are co-enriched at similar target genes. (**a**) ChIP-qPCR analysis showing relative enrichment of EBS and CLF at *SOC1*, *EMF1*, and *FLC*. The *TA3* locus serves as a negative control. Bars denote the mean of two independent experiments. (**b**) Venn diagram showing number of genes overlap between EBS with LHP1 (ref 29) and EMF1 (ref 31). (**c-d**) Metplots showing the average H3K27me3 (c) and H3K4me3 levels (d) along the transcription unit of 301 EBS-bound genes co-marked with H3K4me3 and H3K27me3.

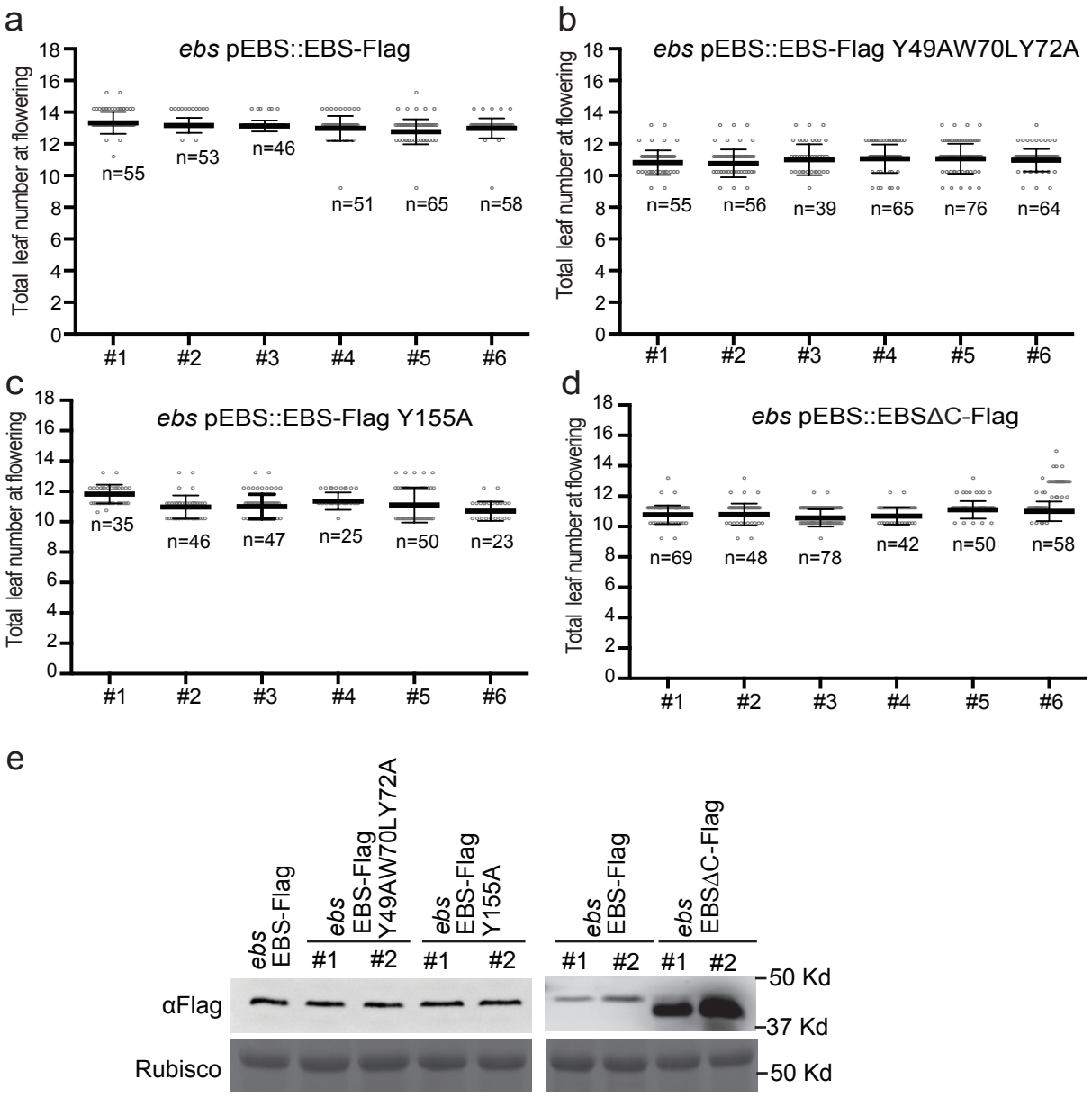

Supplementary Figure 6 Phenotypic analysis of EBS mutants with disrupted H3K4me3 or H3K27me3 binding. (**a-d**) Flowering time analysis of long-day grown plants from 6 independent T_2 *ebs* transgenic plants expressing wild-type EBS-FLAG (a), H3K27me3 binding defective triple mutant EBS Y49A W70A Y72A (b), H3K4me3 binding defective mutant EBS Y155A (c), and C-terminus deletion mutant EBSΔC (d). Black horizontal lines are mean and the error bars represent mean ± SD from the number of plants (indicateb by n) counted for each line (white dots). (**e**) Western blot analysis of protein expression levels from plants indicated in (a-d) using an anti-FLAG antibody. Rubisco serves as a loading control. Two independent lines for each transgene are shown (uncropped images in Supplementary Fig. 8).

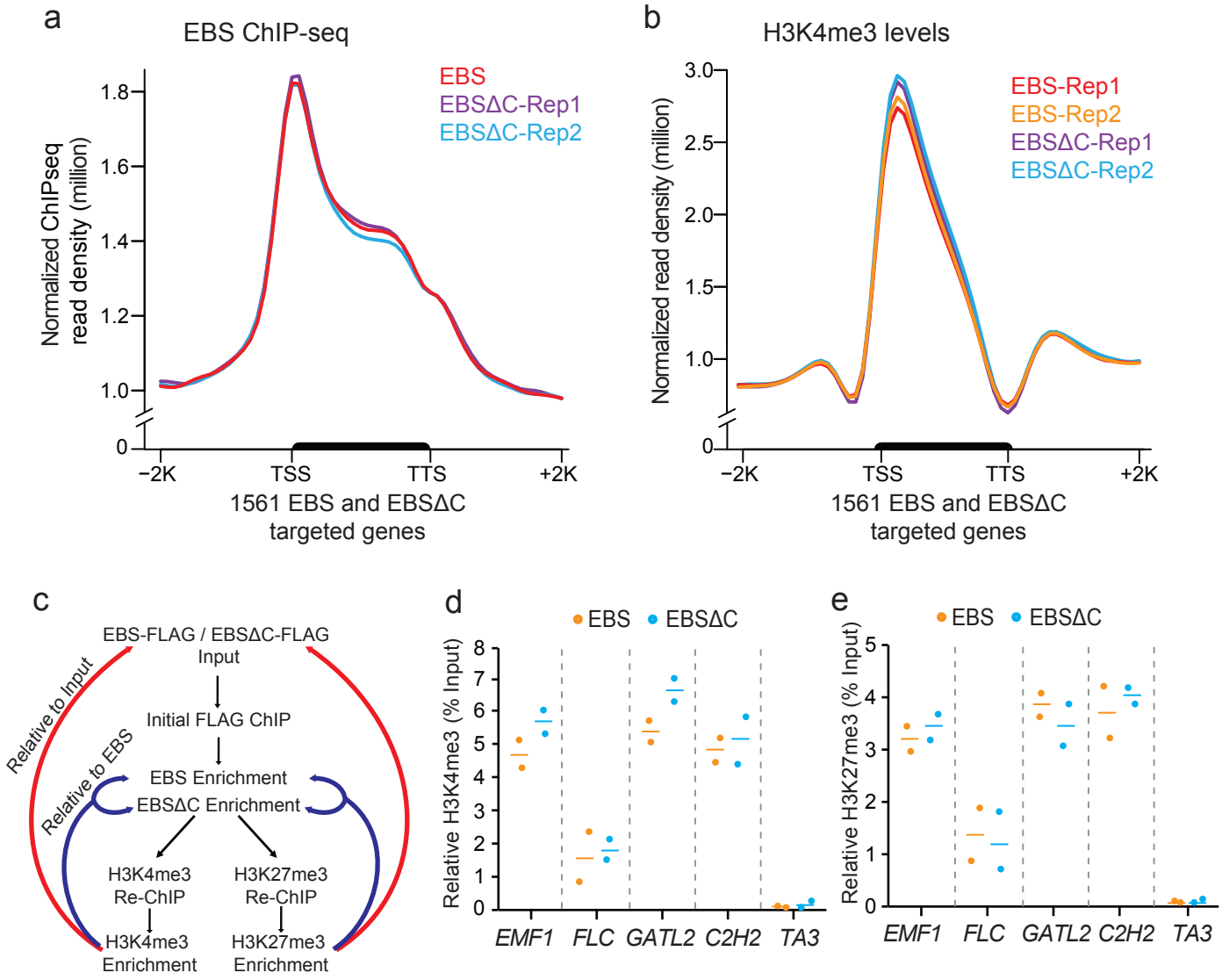

Supplementary Figure 7 Genome-wide H3K4me3 levels in EBS and EBSΔC. (**a-b**) Meta-plot showing the average levels of EBS and EBSΔC occupancy (a) and H3K4me3 levels (b) over EBS and EBSΔC commonly targeted genes in transgenic plants expressing EBS-Flag and EBSΔC-Flag. Two independent biological replicates are shown as Rep1 and Rep2, respectively. TSS, transcription start site; TTS, transcription terminal site. -2K and +2K represent 2kb upstream of TSS and 2kb downstream of TTS, respectively. Y-axis represents the read density after normalization with the total reads. (**c**) Shematic representation of the work flow for the sequential ChIP. (**d-e**) ChIP-qPCR of H3K4me3 (d) or H3K27me3 (e) enrichment relative to input materials in plants expressing EBS-Flag and EBSΔC-Flag. Bars denote the mean of two independent experiments.

Figure 5b

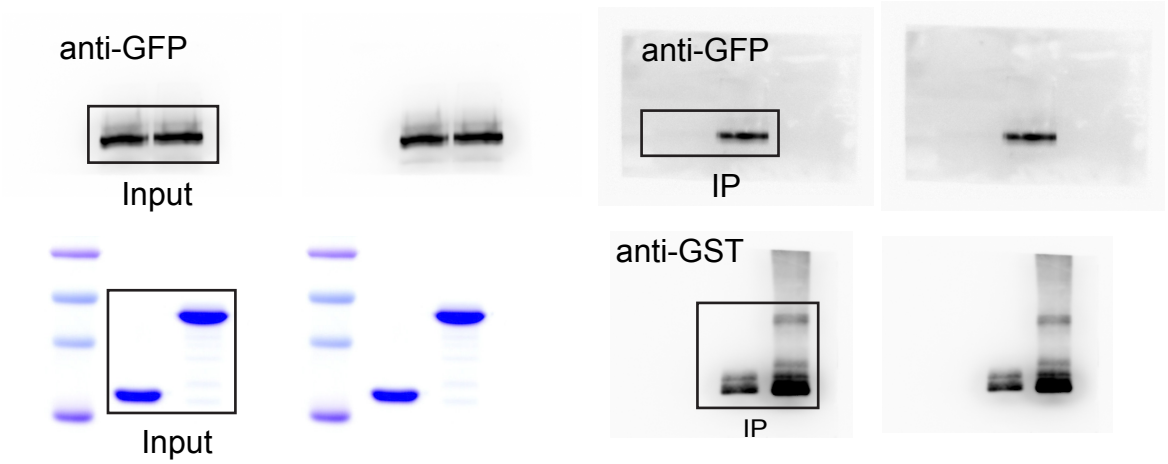

Figure S6e

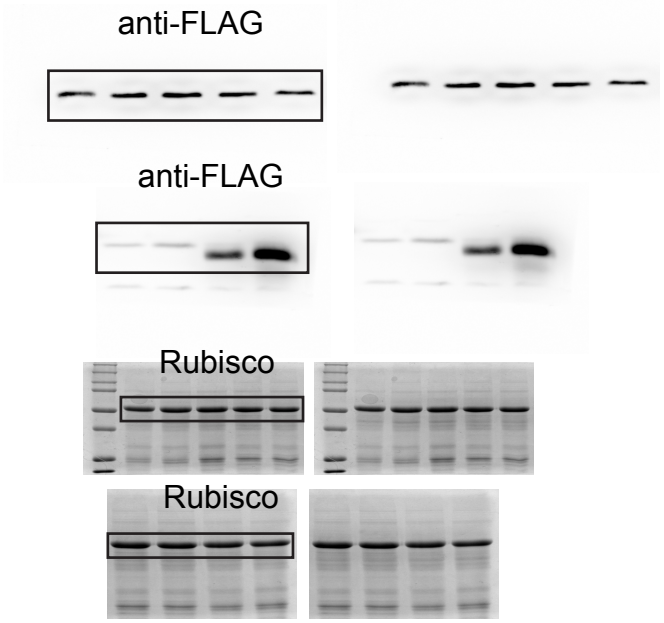

Supplementary Figure 8 Orginal uncropped scans of representative immunoblots displayed in this manuscipt.